



OPEN

SUBJECT AREAS:

COMPUTATIONAL
METHODSMAGNETIC PROPERTIES AND
MATERIALS

Spectrum Gaps of Spin Waves Generated by Interference in a Uniform Nanostripe Waveguide

Qi Wang, Huaiwu Zhang, Guokun Ma, Yulong Liao, Xiaoli Tang & Zhiyong Zhong

Received
21 March 2014Accepted
11 July 2014Published
1 August 2014Correspondence and
requests for materials
should be addressed to
Z.Y.Z. (zzy@uestc.
edu.cn)

State key Laboratory of Electronic Thin Films and Integrated Devices, University of Electronic Science and Technology of China, Chengdu, 610054, China.

We studied spin waves excited by two or more excitation sources in a uniform nanostripe waveguide without periodic structures. Several distinct spectrum gaps formed by spin waves interference rather than by Bragg reflection were observed. We found the center frequency and the number of spectrum gaps of spin waves can be controlled by modulating the distance, number and width of the excitation sources. The results obtained by micromagnetic simulations agree well with that of analytical calculations. Our work therefore paves a new way to control the spectrum gaps of spin waves, which is promising for future spin wave-based devices.

Magnonic crystals, counterparts of photonic crystals, are consisting of periodic magnetic materials¹. The periodic structure affects the spin waves dispersion curve by causing a forbidden band at Brillouin zone boundaries due to Bragg reflection. The first evidence of Bragg reflection of spin wave was presented in a width-modulated nanostripe waveguide². In periodic thin ferromagnetic films, spin waves with gigahertz frequencies can be confined^{1–6}, focused and guided^{7–12}. Such spin waves have wavelengths that are a few orders of magnitude shorter than that of electromagnetic waves at the same frequency. These properties make magnonic waveguides (MWs) promising candidates for nanoscale signal processing and information transfer devices such as filters^{2–4}, delay lines^{13,14}, and storage elements¹⁵.

In recent years, many MWs designs have been presented and tested to realize signal processing functions. Usually, these MWs are fabricated with different magnetic materials^{16,17}, with different structures^{2,3,6} or with a local Oersted fields¹³. However, fabrication of periodic nanostructures involves high-precision electron-beam lithography which is very complex and expensive. On the other hand, the spin waves in these periodic structures always reflect at the Brillouin zone boundaries, resulting in an increase of the transmission loss and a decrease of the propagation distance. Therefore, how to manipulate spin waves in uniform waveguides is still an intriguing project so far.

In this paper, we present a new way to manipulate spin waves by interference in a uniform waveguide rather than by traditional Bragg reflection in periodic structure waveguide. The simple uniform waveguide with two or more excitation sources (ESs) is studied. The spin waves, excited by different ESs, interfere constructively and destructively in the uniform waveguide and form conduction bands and forbidden bands. The physical origin of spectrum gaps in such multi-sources waveguide and the relations between the center frequency of spectrum gaps and the distance, number and width of ESs are studied in detail by numerical micromagnetic simulations and analytical calculations.

Results

The sketch of the present study is shown in Fig. 1. The initial magnetization along the longitudinal axis, the backward volume magnetostatic spin waves (BVMSW) are studied in the following and the analogous results in the Damon–Eshbach (DE) mode can be found as Supplementary Fig. S4 online. As a reference, we simulate a same dimension waveguide with a single ES. The frequency spectrum, transmission characteristic and dispersion curve of spin waves are displayed in Fig. 2 (a),(b), (c), respectively. The spin wave transmission isn't allowed below 12 GHz, which attributes to the nanostripe width confinement^{18,19}. For the waveguide with a single ES, there is no spectrum gap above 12 GHz. On the contrary, there are two spectrum gaps for the two ESs waveguide as shown in Fig. 2 (d) – (f), where the distance and width of the two ESs are $D = 28$ nm and $W = 2$ nm (the length of cell), respectively.

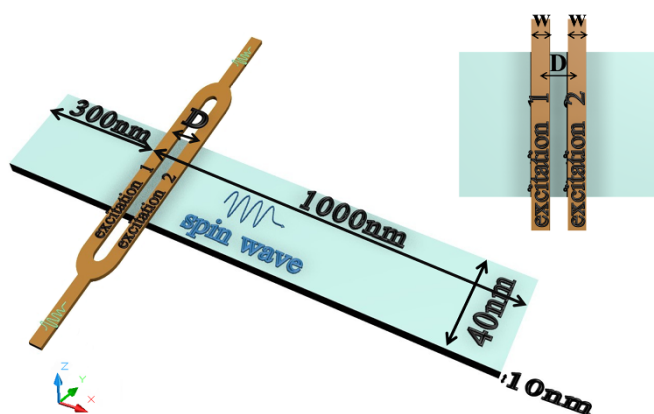


Figure 1 | Schematic of waveguide with two excitation sources. D and W are the distance and width of the ESs, respectively.

To understand such spectrum gaps features, we plot the dispersion curves of waveguide with single and two ESs in Fig. 2(c) and (f), respectively. The dispersion curves obtained by micromagnetic simulations agree with that of analytical calculations^{20–22} (see Fig. 2(c)). We can observe two distinct spectrum gaps in Fig. 2(d) – (f). The wave vectors and center frequencies of the two spectrum gaps are $k_1 = 0.1135 \text{ nm}^{-1}$, $k_2 = 0.3371 \text{ nm}^{-1}$ and $f_1 = 19.53 \text{ GHz}$, $f_2 = 97.17 \text{ GHz}$, respectively. In terms of the dispersion characteristics, the spectrum gaps are not caused by Bragg reflection. The slopes of the dispersion curve at the edges of the spectrum gaps keep stable shown in Fig. 2(f), whereas the Bragg reflection caused the slopes decrease obviously^{2,15,23}.

In order to quantitatively elucidate the physical origin of the spectrum gaps, we introduced the expression of dynamic magnetization of m_z component for a stripe waveguide^{24–26}

$$m_z(|x|) = -\frac{4\pi i}{L} h_{|k|sz} \exp(i|kx|) \quad (1)$$

where L is the thickness of waveguide, the magnitude h_{ksz} is the spatial Fourier component of microwave field ($h_{sz}(x)$) corresponding to the wave vector k . In consideration of the interference between the two ESs, the resultant magnitude of the spin waves which are independently excited by different ESs is obtained:

$$m_{z(\text{sum-two})}(x) = -\frac{4\pi i}{L} h_{ksz} \exp(ikx)[1 + \exp(ikD)] \quad (2)$$

Note that we only consider the area far away from the antenna ($x \gg D$) and the excitation fields are identical (amplitude, phase, direction and so on). The spin waves destructively interfere and disappeared ($m_{z(\text{sum-two})} = 0$) when the wavelength meets $D = (2n + 1)/2 \times \lambda$, ($n = 0, 1, 2, 3, 4, \dots$), where $\lambda = 2\pi/k$ is the wavelength of spin wave. The condition for destructive interference is similar to double-slit interference in light. We calculated the wavelengths corresponding to the center frequencies of spectrum gaps. For 19.53 GHz and 97.17 GHz, the wavelengths are $\lambda_{19.53\text{GHz}} = 55 \text{ nm}$ and $\lambda_{97.17\text{GHz}} = 18.6 \text{ nm}$, respectively. Taking into account the distance ($D = 28 \text{ nm}$) between the ESs, we found $D \approx 1/2 \times \lambda_{19.53\text{GHz}}$ and $D \approx 3/2 \times \lambda_{97.17\text{GHz}}$. Therefore, we can conclude that the spectrum gaps are mainly generated by the interference between the spin waves excited by different ESs. The spin waves, which meet the condition of destructive interference, can't propagate along waveguide and form spectrum gaps.

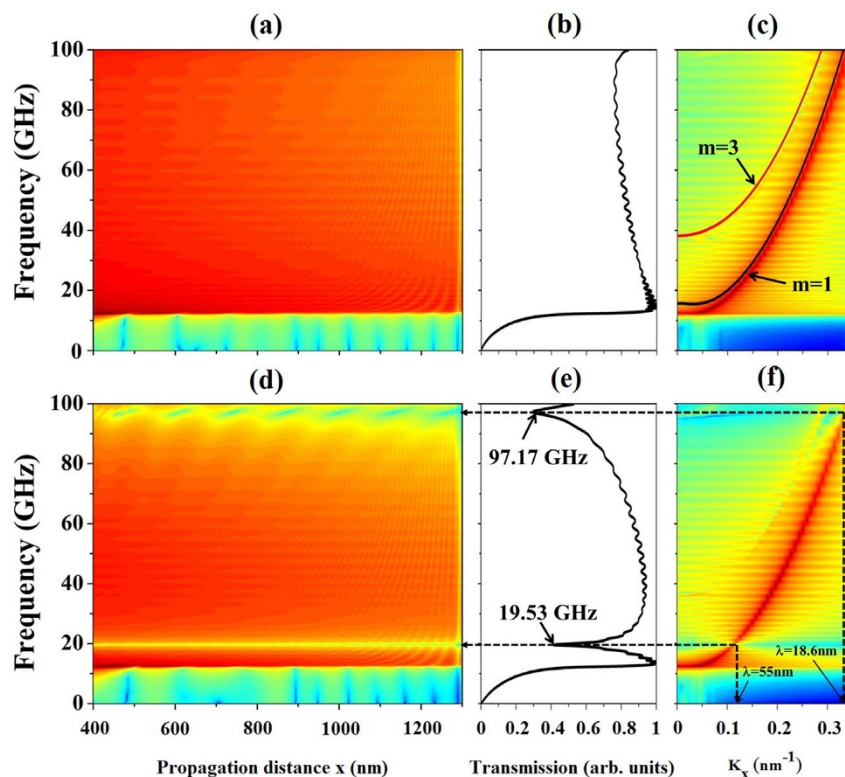


Figure 2 | Characteristics of two uniform waveguides with different number ESs. The top and bottom panels correspond to waveguides with one and two ESs, respectively. (a), (d) The frequency spectra obtained from FFT of M_z . (b), (e) Spin wave transmission characteristics obtained by means of the spin waves intensity of a range of the waveguides (from 1000 nm to 1200 nm). The inset frequencies indicate the positions of the spectrum gaps. (c), (f) The dispersion curves of the first and third modes obtained by micromagnetic simulation and analytical calculation (the red and black line in Fig. 2(c)). The black dotted lines denote the positions of the spectrum gaps and the corresponding wave vectors k_x . The inset wavelengths correspond to the wave vectors.

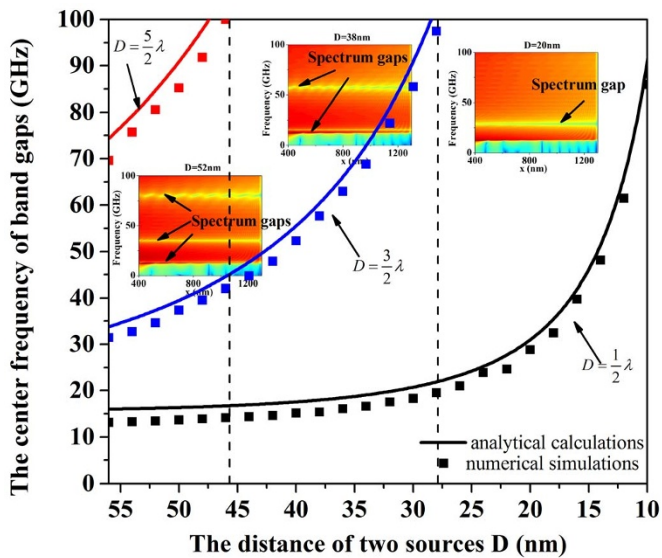


Figure 3 | The center frequencies of spectrum gaps determined from micromagnetic simulation (square shape) and compared to the analytical calculation (line) for the different distances (D) of ESs. The insets depict the frequency spectra for $D = 20$ nm, $D = 38$ nm and $D = 52$ nm. The black, blue and red line indicate the center frequencies of spectrum gaps caused by the first ($D = 1/2 \times \lambda$), second ($D = 3/2 \times \lambda$) and third ($D = 5/2 \times \lambda$) order interferences, respectively.

In order to obtain the dependence of the center frequency of spectrum gaps on the distance of ESs, we recorded and analyzed the frequency spectra at different distance of 10–56 nm. The results of these simulations agree with that of analytical calculations, as shown in Fig. 3. At $D = 20$ nm, there is only one spectrum gap (the center frequency 28.8 GHz) in the frequency range from 0 to 100 GHz, the wavelength of the center frequency is about 39.1 nm ($D \approx 1/2 \times \lambda_{28.8\text{GHz}}$). More spectrum gaps can be found in this frequency range as the distance increases. The spectrum gaps at higher frequencies correspond to higher order interferences.

The above discussions about two ESs waveguide prove that the generation of spectrum gaps of spin waves is caused by interference. We will further explore the effect of the number of ESs in this section. The transmission characteristic and dispersion curve show a distinct spectrum gap for the three ESs in Fig. 4 (a) and (b). The wave vector of the spectrum gap is 0.2094 nm^{-1} , the corresponding wavelength

can be calculated $\lambda = 2\pi/k = 29.99 \text{ nm}$. The wavelength doesn't meet the principle obtained in two ESs interference. Taking multi-sources interference into account, the resultant magnitude of the spin waves can be expressed as:

$$m_z(\text{sum-multi})(x) = -\frac{4\pi i}{L} h_{kxz} \exp(ikx) [1 + \exp(ikD) + \exp(i2kD) + \dots + \exp(i(N-1)kD)] \quad (3)$$

where N is the number of ESs. When the sum of spin waves intensity equal to zero ($m_z(\text{sum-multi}) = 0$) the interference is destructive. Thus, we can drive a simple rule $ND = n\lambda$ ($n = 1, 2, 3, 4, 5, \dots$). If this rule is met, the interferences of the spin waves will be destructive and the spectrum gaps will be observed in the dispersion curves. For the three ESs ($N = 3$), the wavelength corresponding to the spectrum gap is $\lambda = 29.99 \text{ nm}$. The result is closely correlated with the analytical calculations ($\lambda = ND = 3 \times 10 = 30 \text{ nm}$). The calculation (line) and micromagnetic simulations (dot) results are presented in Fig. 4 (c). All the data is obtained by changing the number of the ESs. The distance ($D = 10 \text{ nm}$) and width ($W = 2 \text{ nm}$) of the ESs are fixed during the process. Figure 4(c) shows that the developed theory above of multi-sources interference gives good quantitative description of the micromagnetic simulations.

Discussion

All the results and discussions above are based on the fixed width of ESs ($W = 2 \text{ nm}$) which is less than the exchange length of the simulated magnetic material. However, it is very difficult to be fabricated using the existing lithography tools. Hence, the different widths of the ESs must be considered. Figure 5(a) shows the sketch of a single ES with width W . The single ES can be viewed as many narrower ESs with width λ_{ex} , where λ_{ex} is the exchange length. Each portion of the ES will act as a source of spin waves. The multi-sources waveguide have been discussed in above sections. In this condition, the center distance of the nearest neighbor ESs is $D = \lambda_{\text{ex}}$ and the number of the ESs is $N = W/\lambda_{\text{ex}}$. The condition of destructive interference is

$$\lambda = \frac{ND}{n} = \frac{\frac{W}{\lambda_{\text{ex}}} \times \lambda_{\text{ex}}}{n} = \frac{W}{n} \quad (n = 1, 2, 3, 4, 5, \dots) \quad (4)$$

We compare the calculated (line) and micromagnetic simulated (dot) data in Fig. 5(b). The results show that the developed approximate theory above of wider ES gives good quantitative description of the data of micromagnetic simulations.

At last, we consider general situations in a multi-sources waveguide. Figure 6 shows the frequency spectra and transmission char-

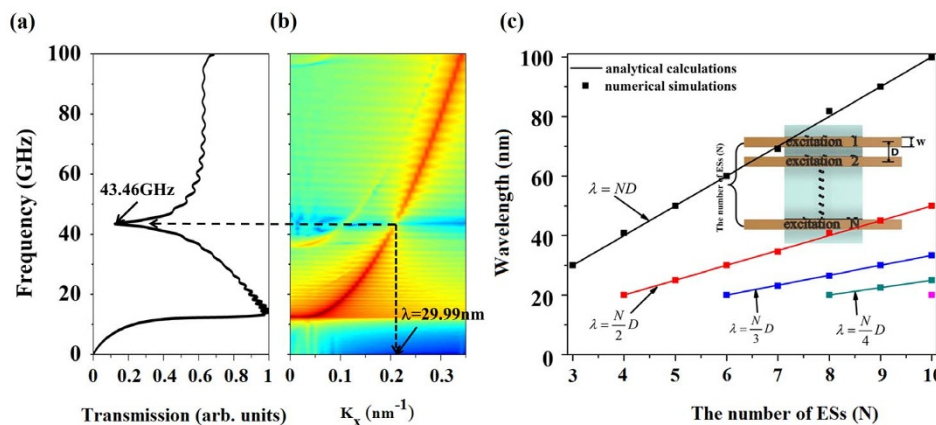


Figure 4 | (a) The transmission characteristic of spin wave obtained by meaning the spin wave intensity of a range of the waveguide (from 1000 nm to 1200 nm) for three ESs. The inset frequency indicates the position of the spectrum gap. (b) The dispersion curve of spin wave. The dashed black dot lines denote the frequency and wave vector of spectrum gap. (c) The numerical simulations (dot) and analytical calculations (line) results for the different number of ESs. The inset indicates the sketch of multi-sources waveguide.

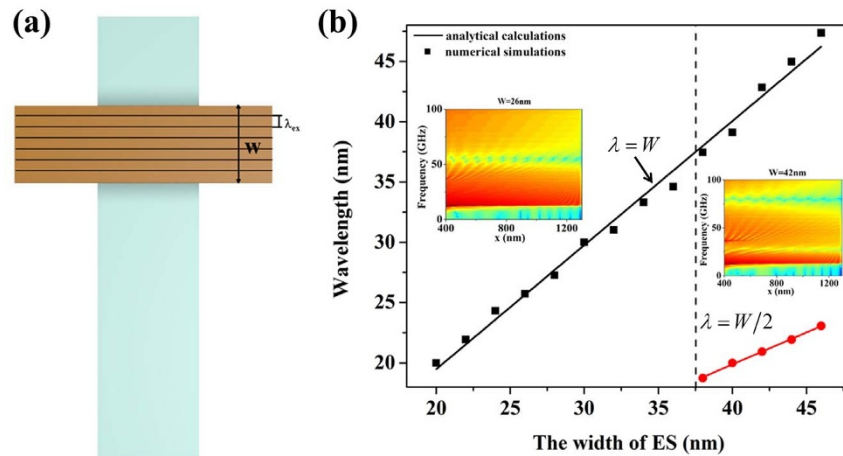


Figure 5 | (a) The sketch of a single ES with width W . (b) The numerical simulations (dot) and analytical calculations (line) results dependencies of the width of ESs. The insets indicate the frequency spectra of spin wave for $W = 26$ nm and $W = 42$ nm, respectively.

acteristics for different ESs. The frequency spectra with only one spectrum gap for the single ES with $W = 20$ nm is shown in Fig. 6(a) and with two spectrum gaps for the two ESs with $W = 2$ nm and $D = 40$ nm is shown in Fig. 6(b). As we expected, there are three spectrum gaps for two ESs with $W = 20$ nm and $D = 40$ nm, as shown in Fig. 6(c). The highest one is caused by the interference of the single ES with $W = 20$ nm and the lower two are caused by the interference of two ESs with $W = 2$ nm and $D = 40$ nm. The transmission characteristics of spin waves for different ESs are shown in Fig. 6(d). The blue line ($W = 20$ nm and $D = 40$ nm) is the superposition of the black (single ES $W = 20$ nm) and red ($W = 2$ nm and $D = 40$ nm) lines. We have previously discussed

the effect of the distance and width of the ESs on spectrum gaps, respectively. Therefore, we could easily tune the spectrum gaps for a general situation in multi-sources waveguide.

In conclusion, we performed micromagnetic simulations of the spin wave in a uniform waveguide with several ESs. The appearance of spectrum gaps was clearly observed in multi-sources waveguide. The spectrum gaps are originated from the interference between the different spin waves independently excited by different ESs. Moreover, the position and the number of spectrum gaps can be manipulated by the distance, number and width of ESs. Although our calculations were done in nanometer, similar interference conditions could be obtained in micrometer (see Supplementary Fig. S1–

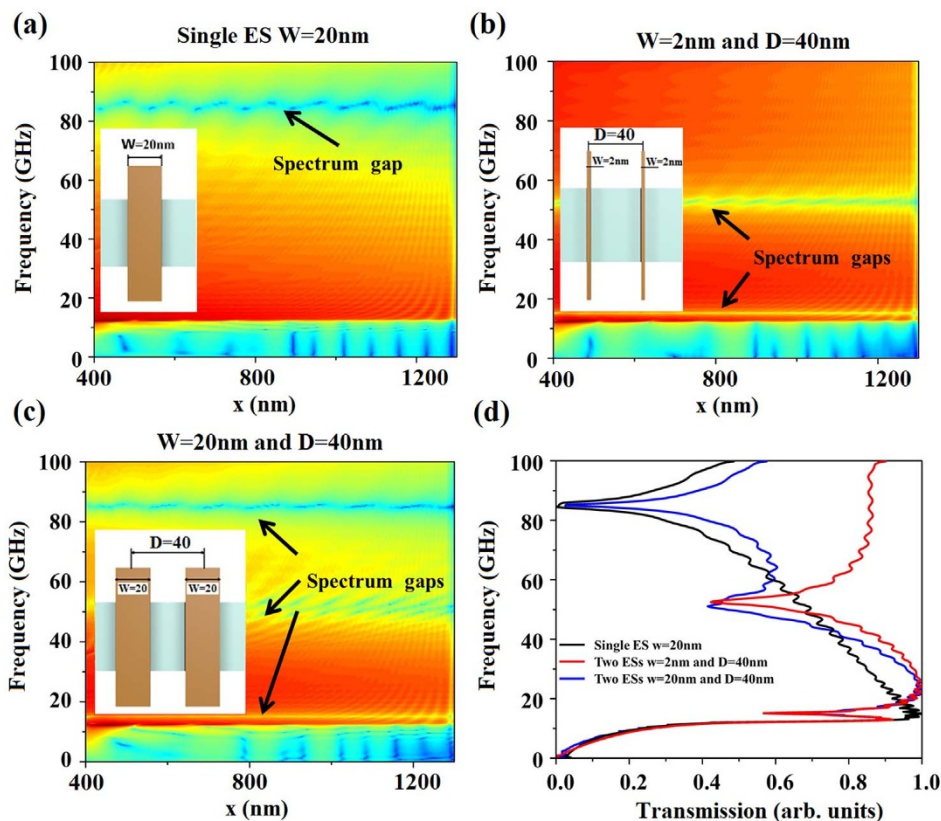


Figure 6 | The frequency spectra of spin wave for (a) single ES with $W = 20$ nm, (b) two ESs with $W = 2$ nm and $D = 40$ nm, (c) two ESs with $W = 20$ nm and $D = 40$ nm. The insets indicate the sketch of different ESs. (d) The transmission characteristics of spin waves for different ESs.



S3). This work is expected to provide an alternative way to manipulate spin waves besides traditional magnonic crystals.

Methods

The waveguide used in our numerical simulations is sketched in Fig. 1. The 10 nm thick permalloy waveguides with width ranging from 40 to 1000 nm and length ranging from 1300 to 6000 nm were studied in our works. Considering the slow calculation speed, we mainly studied the waveguide with width of 40 nm and length of 1300 nm. Others sizes were provided in the Supplementary Fig. S1–S3 online. Simulations were performed using OOMMF code [A version of the OOMMF code used is 1.2a5 (2012)] to solve the Landau-Lifshitz-Gilbert equation. The parameters are as follows: the exchange constant $A = 13 \times 10^{-12}$ J/m, the saturation magnetization $M_s = 8.6 \times 10^5$ A/m, the damping constant $\alpha = 0.01$ and the cell size $2 \times 2 \times 10$ nm³. The damping parameter α in the boundary areas (~ 20 nm on each side) was increased more than fifty times to prevent the reflection at the ends of the structure. In order to excite spin waves with a wide frequency range, we applied a sinc function excitation with frequencies ranging from 0 to 100 GHz and an amplitude of 1.0 T. The excitation, after through the input antenna, was separated into two identical ES (amplitude, direction and phase).

- Kruglyak, V. V., Demokritov, S. O. & Grundler, D. Magnonics. *J. Phys. D: Appl. Phys.* **43**, 264001 (2010).
- Lee, K.-S., Han, D.-S. & Kim, S.-K. Physical origin and generic control of magnonic band gaps of dipole-exchange spin waves in width-modulated nanostrip waveguides. *Phys. Rev. Lett.* **102**, 127202 (2009).
- Kim, S.-K., Lee, K.-S. & Han, D.-S. A gigahertz-range spin-wave filter composed of width-modulated nanostrip magnonic-crystal waveguides. *Appl. Phys. Lett.* **95**, 082507 (2009).
- Ma, F. S. *et al.* Micromagnetic study of spin wave propagation in bicomponent magnonic crystal waveguides. *Appl. Phys. Lett.* **98**, 153107 (2011).
- Duerr, G., Thurner, K., Topp, J., Huber, R. & Grundler, D. Enhanced transmission through squeezed modes in a self-cladding magnonic waveguide. *Phys. Rev. Lett.* **108**, 227202 (2012).
- Chumak, A. V. *et al.* Spin-wave propagation in a microstructured magnonic crystal. *Appl. Phys. Lett.* **95**, 262508 (2009).
- Demidov, V. E., Demokritov, S. O., Rott, K., Krzysteczko, P. & Reiss, G. Mode interference and periodic self-focusing of spin waves in permalloy microstrips. *Phys. Rev. B* **77**, 064406 (2008).
- Topp, J., Podbielski, J., Heitmann, D. & Grundler, D. Internal spin-wave confinement in magnetic nanowires due to zig-zag shaped magnetization. *Phys. Rev. B* **78**, 024431 (2008).
- Clausen, P. *et al.* Mode conversion by symmetry breaking of propagating spin waves. *Appl. Phys. Lett.* **99**, 162505 (2011).
- Demidov, V. E. *et al.* Transformation of propagating spin-wave modes in microscopic waveguides with variable width. *Phys. Rev. B* **79**, 054417 (2009).
- Mansfeld, S. *et al.* Spin wave diffraction and perfect imaging of a grating. *Phys. Rev. Lett.* **108**, 047204 (2012).
- Choi, S., Lee, K.-S. & Kim, S.-K. Spin-wave interference. *Appl. Phys. Lett.* **89**, 062501 (2006).
- Chumak, A. V., Neumann, T., Serga, A. A., Hillebrands, B. & Kostylev, M. P. A current-controlled, dynamic magnonic crystal. *J. Phys. D: Appl. Phys.* **42**, 205005 (2009).
- Ustinov, A. B., Drozdovskii, A. & Kalinikov, B. A. Multifunctional nonlinear magnonic devices for microwave signal processing. *Appl. Phys. Lett.* **96**, 142513 (2010).
- Chumak, A. V. *et al.* Storage-recovery phenomenon in magnonic crystal. *Phys. Rev. Lett.* **108**, 257207 (2012).
- Neusser, S. & Grundler, D. Magnonics: spin waves on the nanoscale. *Adv. Mater.* **21**, 2927–2932 (2009).
- Wang, Z. K. *et al.* Observation of frequency band gaps in a one-dimensional nanostructured magnonic crystal. *Appl. Phys. Lett.* **94**, 083112 (2009).
- O’Keeffe, T. W. & Patterson, R. W. Magnetostatic surface-wave propagation in finite samples. *J. Appl. Phys.* **49**, 4886–4895 (1978).
- Choi, S., Lee, K.-S., Guslienko, K. Yu. & Kim, S.-K. Strong radiation of spin waves by core reversal of a magnetic vortex and their wave behaviors in magnetic nanowire waveguides. *Phys. Rev. Lett.* **98**, 087205 (2007).
- Kittel, C. Excitation of spin waves in a ferromagnet by a uniform rf field. *Phys. Rev.* **110**, 1295–1297 (1958).
- Guslienko, K. Yu., Demokritov, S. O. & Hillebrands, B. Effective dipolar boundary conditions for dynamic magnetization in thin magnetic stripes. *Phys. Rev. B* **66**, 132402 (2002).
- Guslienko, K. Yu. & Slavin, A. N. Boundary conditions for magnetization in magnetic nanoelements. *Phys. Rev. B* **72**, 014463 (2005).
- Zivieri, R. *et al.* Bragg diffraction of spin waves from a two-dimensional antidot lattice. *Phys. Rev. B* **85**, 012403 (2012).
- Kostylev, M. P. *et al.* Resonant and nonresonant scattering of dipole-dominated spin waves from a region of inhomogeneous magnetic field in a ferromagnetic film. *Phys. Rev. B* **76**, 184419 (2007).
- Schneider, T., Serga, A. A., Neumann, T. & Hillebrands, B. Phase reciprocity of spin-wave excitation by a microstrip antenna. *Phys. Rev. B* **77**, 214411 (2008).
- Demidov, V. E. *et al.* Excitation of microwaveguide modes by a stripe antenna. *Appl. Phys. Lett.* **95**, 112509 (2009).

Acknowledgments

This paper is supported by the National Nature Science Foundation of China under Grant Nos. 61271037, 61071028, and 61271038, and the RFDP under No 20120185110029.

Author contributions

Q.W., H.W.Z. and Z.Y.Z. conceived and supervised the research. Q.W. conducted the micromagnetic simulations and wrote the manuscript. G.K.M., Y.L.L. and X.L.T. made the theoretical analysis. All the authors discussed the results.

Additional information

Supplementary information accompanies this paper at <http://www.nature.com/scientificreports>

Competing financial interests: The authors declare no competing financial interests.

How to cite this article: Wang, Q. *et al.* Spectrum Gaps of Spin Waves Generated by Interference in a Uniform Nanostripe Waveguide. *Sci. Rep.* **4**, 5917; DOI:10.1038/srep05917 (2014).



This work is licensed under a Creative Commons Attribution-NonCommercial-NoDerivs 4.0 International License. The images or other third party material in this article are included in the article’s Creative Commons license, unless indicated otherwise in the credit line; if the material is not included under the Creative Commons license, users will need to obtain permission from the license holder in order to reproduce the material. To view a copy of this license, visit <http://creativecommons.org/licenses/by-nc-nd/4.0/>